How memory and adaptation cost shape cell phenotypic dynamics in response to fluctuating environments

Paras Jain[a,b], **Mohit Kumar Jolly**[a,1], **and Jason T. George**[b,c,d,e,1]

[a]Department of Bioengineering, Indian Institute of Science, Bangalore 560012
[b]Department of Biomedical Engineering, Texas A&M University, College Station, TX 77843
[c]Translational Medical Sciences, Texas A&M Health Science Center, Houston, TX 77030
[d]Center for Theoretical Biological Physics, Rice University, Houston, TX 77005
[e]Hematopoietic Biology and Malignancy, MD Anderson Cancer Center, Houston, TX 77030

Cells invariably encounter unpredictable changes in their microenvironment and undergo adaptation by orchestrating considerable alterations in their molecular states that often result in appreciable phenotypic changes. The timescale of molecular and, therefore, cellular adaptation depends on how quickly the memory of past environmental encounters is lost (and therefore forgotten) by the cell (e.g., degradation rate of proteins unfavorable to the current environment). Here, we study the dynamical implications of two distinct memory mechanisms on cellular responses to a changing environment. The two phenomenological models considered are – 1) Undated memory, wherein each prior environmental exposure has an equal probability to dissipate in the next time step, and 2) Dated memory, wherein each experience is dated and erased according to its order of encounter. We observed that while dated memory leads to faster adaptation in single-step environmental perturbations and helps in quick recovery of cellular benefit, the optimal memory type in the periodic environment depends on the period and cell memory capacity. However, both memory types confer comparable cellular benefits in stochastic environments. We extend the results with these memory types to show how the cost incurred during cellular adaptation (e.g., energetic cost of mRNA and protein production) improves cellular decision-making by delaying the phenotypic response until enough environmental change is experienced by the cells. However, such delayed adaptation proves detrimental to the cells under one-step environmental perturbations. Together, these results elucidate the intricate roles of memory and adaptation cost in phenotypic adaptation in fluctuating environments.

Biophysics | Phenotypic Adaptation Dynamics | Applied Stochastic Processes

Correspondence: ***mkjolly@iisc.ac.in, jason.george@tamu.edu***

Introduction

Phenotypic adaptation is a defining response of cellular systems navigating variable environmental conditions. Studies focused on disparate biological contexts spanning bacterial, yeast, and cancer systems have extensively characterized cellular phenotypic changes to steady environments and single environmental switches. Only recently has there been an increasing focus on cellular responses to fluctuating environments (1–5). Environmental fluctuations drive cellular adaptation across many timescales. For example, seconds-to-minutes scale changes in nutrient gradients drive bacterial motility, while hours-to-days scale changes in oxygen concentration induce distinct cellular growth phenotypes in cancer cells (6–8). It has been shown empirically that dynamic environmental conditions produce a cellular responses that can differ significantly from what would be expected by taking a suitable weighted average of responses in static environments conditions (4). Moreover, these responses to dynamic environmental changes result from orchestration of cellular action based on past environmental encounters, representing an imprinting or 'cellular memory' (5, 9, 10). A more complete understanding of cellular behavior therefore necessitates understanding cellular responses to fluctuating environmental conditions.

Prior theoretical models have improved our understanding of cellular responses in changing environments (11, 12). While considering long-term population-level survival under spontaneous versus adaptive phenotypic transitions in stochastic environments, Kussell and Leibler identified a threshold environmental fluctuation rate below which adaptive switching is more beneficial than spontaneous switching (bet-hedging) (13). Subsequent modeling identified changes in adaptation dynamics based on whether or not adaptation was driven exclusively by past environmental encounters (14). Further, hysteresis in cell-state switching has been observed and shown to confer higher growth benefit to cells navigating stochastic, but not periodic environments (15). While the above studies have contributed to our understanding of population-level adaptation behavior under dynamic environments, the relationship between intracellular responses to changing environments and their consequent effects on cellular adaptation were not explored (16–18).

A myriad of conserved intracellular responses exist and result from diverse environmental changes (stressors). For example, expression of Lac operon genes in Escherichia coli during nutrient shift from glucose to lactose; and expression of drug efflux pump MDR1 in acute myeloid leukemic cells upon exposure to vincristine drug (19–22). Importantly, once the environment switches to normal conditions, the relaxation time of the biochemical reaction network (that mediates stress response) to its basal state dictates cellular memory of the past environmental experiences. For example, in *E. coli* cells, dilution of Lac proteins levels on subsequent divisions post lactose exposure fades the cell memory and add lag and

DRAFT

recovery times to cell growth upon lactose re-exposure. (19). Similarly, residual abundance of MDR1 levels in cancer cells post vincristine pulsed treatment enhanced their survival on drug re-exposures(20). Thus, persistence of cellular memory depends largely on the determinants of relaxation times for biochemical reaction networks (23, 24).

One of the important factors determining biochemical network relaxation times is the degradation profiles (rates) of the networks component biomolecules (mRNAs and proteins) (17, 23). Rapid turnover of mRNAs benefits cells navigating dynamic environments by freeing up translational machinery for synthesizing proteins essential for navigating each environmental state (25, 26). However, since degradation of mRNAs and proteins comprise either one-step or multi-step processes, the turnover rate may depend on the number of the intermediate steps involved (27–30). The precise implications of variablility in relaxation times and subsequent memory erasure on cellular adaptation in fluctuating environments therefore represents an open question.

Another factor that affects cellular adaptation is the energetic cost of *de-novo* synthesis of bio-molecules. Cellular maintenance of a particular phenotypic state in steady environments relies on persistent biomolecular synthesis and degradation, largely owing to negative feedback (31, 32). These non-equilibrium steady states require a constant cellular energy influx, and thus there is a trade-off between energy consumption and the ability to accurately detect the environment (31, 33). In fluctuating environments, cells are therefore limited in their ability to optimally navigate all possible environments – constrained by the associated energetic demands of protein production – and perform *de-novo* synthesis of essential proteins in response to the inferred environment (34, 35). Thus, every environment switch may burden the cell with additional energetic costs for adaptation. How this cost of adaptation in a fluctuating environment affects the long-term growth of cells is yet to be explored.

Here, we present a generalized phenomenological model of cellular adaptation in fluctuating environments that account for the above features. Specifically, we frame adaptation dynamics as an optimal decision process whereby cells leverage a molecularly encoded memory of past environmental exposures to inform the progression of their phenotypic states over time, and we develop analytical theory to characterize the above adaptive response. The model accounts for 1) one-step 'undated memory' and multi-step 'dated memory' decay, and 2) non-negligible energetic costs of phenotypic adaptation. We demonstrate that while, dated memory results in efficient cellular navigation of one-step environmental perturbations, the optimal memory scheme in periodic environments depend on memory capacity and the period of environmental switching. Such differences in the optimal memory scheme vanish in stochastic environments. Surprisingly, the addition of phenotypic adaptation costs often delays extraneous cellular adaptation in fluctuating environments, thereby resulting in enhanced overall growth. Overall, our study highlights the non-intuitive roles of cellular memory and adaptation cost in dictating cellular adaptation and benefits in variable environments.

Model Development

Optimal phenotypic states in fluctuating environments. We adapted and generalized the stochastic optimal cellular decision model developed by (10). In particular, we considered a discrete-time model where a cell experiences either a beneficial/high (e.g., nutrient) environment (E-high, E^h) or detrimental/low (E-low, E^l) environment at each time step (Figure 1A, B). The cell can reside in one of the two phenotypic states, S^h and S^l, which are preferred in E^h and E^l environments, respectively. Cellular benefit, which in our model represents energetic availability for proliferation and survival is denoted by $r^{\pm}_{l,h}$, with subscript indicating the cell state S and superscript denoting whether the cell state S matches $(+)$ or mismatches $(-)$ with the environment E. For example, a proper match of cell state S^l with the environment E^l (resp. S^h with E^h), results in enhanced benefit r^+_l (resp. r^+_h). However, a mismatch, S^l with E^h (resp. S^h with E^l) result in a reduced benefit r^-_l (res. r^-_h) (Figure 1A).

The cell can switch between S^h and S^l cell states based on the memory of past environment occurrences to maximize its average benefit in the upcoming environment encounter. Furthermore, as cell state switching involves adaptation at multiple intracellular levels, we also incorporate a cost of adaptation - c_{lh} and c_{hl} as the costs for $S^l \to S^h$ and $S^h \to S^l$ transitions, respectively.

Letting E_n denote the environment and S_n the cell state at time n, the benefit accrued by the cell is given by:

$$R_n = \begin{cases} r^+_h \mathbf{1}_{E_n=E^h} + r^-_h(1-\mathbf{1}_{E_n=E^h}), & S_n = S_{n-1} = S^h \\ r^+_h \mathbf{1}_{E_n=E^h} + r^-_h(1-\mathbf{1}_{E_n=E^h}) - c_{lh}, & S_n = S^h, S_{n-1} = S^l \\ r^+_l(1-\mathbf{1}_{E_n=E^h}) + r^-_l \mathbf{1}_{E_n=E^h} - c_{hl}, & S_n = S^l, S_{n-1} = S^h \\ r^+_l(1-\mathbf{1}_{E_n=E^h}) + r^-_l \mathbf{1}_{E_n=E^h}, & S_n = S_{n-1} = S^l, \end{cases} \quad \textbf{(1)}$$

where, $\mathbf{1}_{X_n=X^h}$ is usual indicator function and clearly $\mathbb{E}\left[\mathbf{1}_{X_n=X^h}\right] = \mathbb{P}\left(X_n = X^h\right)$. We denote $p \equiv \mathbb{P}\left(E_n = E^h\right)$ to be the *environmental state*, or probability of the E^h environment in stochastically fluctuating environments.

The differential benefits accrued by each environment-phenotype pair impart a phenotypic preference for each environmental state that depends on p. This preference partitions the environmental landscapes into two groups separated by a critical indifference environment for which each phenotype is equally beneficial. This indifference environment can be calculated by equating the expectations of each pair of values in Eq. (1) having the same phenotype at the previous time step S_{n-1} (See SI Sec. 2.1 and 2.2 for full details). In particular, we have

DRAFT

$$\mathbb{P}\left(E_n = E^h\right)^*_{lh} = p_{lh} = \frac{r_l^+ - r_h^- + c_{lh}}{r_h^+ + r_l^+ - (r_h^- + r_l^-)} \quad \textbf{(2)}$$

In the event that the previous state of the cell is $S_{n-1} = S^l$, and $\mathbb{P}\left(E_n = E^h\right) < p_{lh}$, then $S_n = S^l$ is more beneficial than $S_n = S^h$. Otherwise, $S_n = S^h$ is more beneficial (Figure 1C).

Similarly, the indifference environment, p_{hl}, for S^h to S^l transition can be quantified by replacing c_{lh} with c_{hl} in eq. Eq. (2). Therefore, when $S_{n-1} = S^h$, and $\mathbb{P}\left(E_n = E^h\right) > p_{hl}$, then $S_n = S^h$ is more beneficial; otherwise $S_n = S^l$ is more beneficial (Figure 1C).

As previously defined, p denotes $\mathbb{P}\left(E_n = E^h\right)$ in a stochastic environment. And, in a periodic environment with period T, the $\mathbb{P}\left(E_n = E^h\right)$ at a time instance $n = rT + l$, where r and l being integers, is given by:

$$\mathbb{P}\left(E_n = E^h\right) = p_n = \begin{cases} 0, & 1 \le l \le T_{1/2}^- \\ 1, & T_{1/2}^- < l \le T, \end{cases}$$

where, $T_{1/2}^- = \left\lfloor \frac{T}{2} \right\rfloor$ with the floor function $\lfloor \cdot \rfloor$ giving greatest integer less than or equal to its argument.

We note that for $c_{lh} \ge 0$ and $c_{hl} \ge 0$ the indifference environment $p_{lh} \ge p_{hl}$; and when $c_{lh} = 0$ and $c_{hl} = 0$ we have $p_{lh} = p_{hl} = p_I$. The inequality between p_{lh} and p_{hl} cause hysteresis in cell state switching, i.e., environmental conditions for state switching are different for $S^l \to S^h$ and $S^h \to S^l$ transitions (Figure 1C).

For all the numerical analyses presented in this study we have set $r_h^+ = 2$, $r_h^- = 1$, $r_l^- = 1$, and select values of r_l^+ corresponding to the relevant indifference environments p_I required in each analysis assuming zero adaptation cost (Eq. (2)). Cases having non-negligible adaptation cost are assumed to be symmetric with respect to navigating low-to-high and high-to-low environments (i.e., $c_{lh} = c_{hl}$). Adaptation costs are sampled from the open interval $(0, \min\{r_h^+ - r_l^-, r_l^+ - r_h^-\})$, where $\min(r_h^+ - r_l^-, r_l^+ - r_h^-)$ gives the maximum adaptation cost at or beyond which either $p_{lh} \ge 1$ or $p_{hl} \le 0$.

Memory-driven cellular inference of the environment. In our model cells cannot predict the future environment, but instead make a forecast by estimating p based on a memory of m past environmental encounters. This estimate π_n of p is determined by the relative frequency of E^h environments in the cell memory:

$$\pi_n = \frac{K_n}{m}; \quad K_n = \sum_{n-m+1}^{n} \mathbf{1}_{E_n = E^h},$$

where K_n represents the total number of E^h state experiences in the cell memory at time n. We use 'memory size' and 'memory capacity' interchangeably to refer to the number of past environment instances a cell relies on for decision-making , denoted by 'm'.

Cellular decision making in fluctuating environments. With the estimate π_n of environmental state p, cells apply the following decision-making process to maximize their average benefit at subsequent times (Figure 1C):

$$S_n = \begin{cases} S^h, & \begin{array}{c} S_{n-1} = S^h,\ \pi_{n-1} > p_{hl} \\ or \\ S_{n-1} = S^l,\ \pi_{n-1} > p_{lh} \end{array} \\ S^l, & \begin{array}{c} S_{n-1} = S^h,\ \pi_{n-1} \le p_{hl} \\ or \\ S_{n-1} = S^l,\ \pi_{n-1} \le p_{lh}; \end{array} \end{cases}$$

Dynamics of cellular memory. Cellular memory encoding past environmental experiences arises in a variety of contexts, including, for example, prolonged activation of a signaling cascade post-stimulation and reinforcement of gene expression through chromatin remodeling (9, 23). Here, we focused on general processes in which biomolecule turnover regulates the dynamics of cellular memory in fluctuating environments. Memory updates require the incorporation of more recent signals and the loss of previous ones. We considered two phenomenological means, or memory types, by which a cell may delete previous encounters from its memory: 1) *Undated memory* provides each prior environmental encounter with an equal opportunity to dissipate in the next time step. 2) *Dated memory* erases the oldest memory in the next time step (Figure 1D).

Undated Memory. In this case, all previously recalled environmental experiences have an equal probability of being forgotten irrespective of age. Therefore, at each time step, a random experience from memory gets replaced with a new environmental encounter, as in the endonucleolytic degradation of mRNAs, where rapid mRNA degradation occurs on co-localization with degradation complex (Figure 1Di) (27, 36). We note that fractions $\frac{K_n}{m}$ and $\left(1 - \frac{K_n}{m}\right)$ denote the probabilities of losing a E^h or E^l environmental experience from the memory, respectively. Similarly, p and $(1-p)$ denote the (independent) respective probabilities of gaining a E^h or E^l environmental experience at the next time step. Thus, the dynamics of undated memory can be modeled as a time-homogeneous Markov Chain with states $K_n \in [0, 1, ..., m-1, m]$ and state-transition probabilities given by:

DRAFT

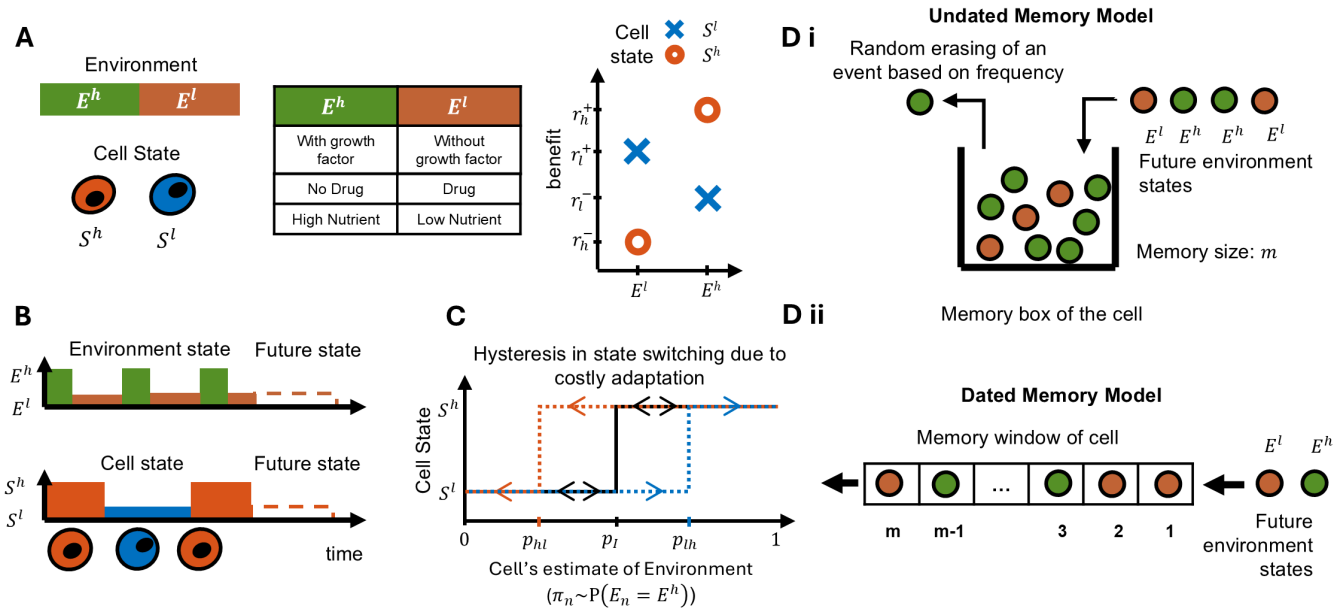

Fig. 1. Environment and cell states, cellular decision making, and cell memory models. A) Consideration that environment can reside one of the two states E^h and E^l. For the two environments, E^h and E^l, optimal cell states S^h and S^l maximize the cell benefit. **B)** A cell navigates a fluctuating environment and optimizes its state to maximize benefit. **C)** Points of cellular decision making to reside in either cell state S^h or S^l based on the cell's estimate of the average environment ($\pi_n \sim \mathbb{P}\left(E_n = E^h\right)$) and maximization of the average cell benefit. p_I represents indifference environment ($\mathbb{P}\left(E_n = E^h\right)^*$) where residing in either cell state is equally beneficial. If there is a cost associated with phenotypic adaptation, then the above indifference environment, p_I, splits into p_{lh} and p_{hl} for $S^l \rightarrow S^h$ and $S^h \rightarrow S^l$ state transitions, respectively. **D)** Proposed cell memory models - Di) Undated Memory, wherein at every discrete time step a random past environmental experience (either E^h or E^l) is erased from the cell memory based on its frequency and the current environmental experience is stored, and Dii) Dated memory, wherein at every discrete time step the oldest environmental experience is erased and the current environmental experience is captured.

DRAFT

$$K_{n+1} = \begin{cases} \textit{next state} & \textit{Probability} \\ K_n, & p\left(\frac{K_n}{m}\right) + (1-p)\left(1 - \frac{K_n}{m}\right) \\ K_n + 1, & p\left(1 - \frac{K_n}{m}\right) \\ K_n - 1, & (1-p)\left(\frac{K_n}{m}\right) \end{cases}$$

Dated memory. In the undated memory model above, each environmental experience encoded in memory has an equal chance to degrade in the next time step. While this assumption may be reasonable for modeling some cellular features, memory erasure may also proceed in age-dependent manner, as in the exonucleolytic degradation of mRNAs, and CRISPR-Cas9-mediated bacterial memory of past bacteriophage infections (Figure 1Dii) (27, 36, 37). Thus, we next considered dated memory where we represent the cell memory by a random vector $\boldsymbol{Z}_n = [E_n\ E_{n-1}\ \ldots\ E_{n-m+1}]$ holding m most recent environment encounters at time n. At each time, the cell memory vector Z_n is updated such that most distant memory (E_{n-m+1} is lost, and a new environmental experience (E_{n+1}) is recorded at time $n+1$.

The transition from vector $\boldsymbol{Z}_n$ to $\boldsymbol{Z}_{n+1}$, can be modeled using a time-homogeneous Markov chain. For example, for $m = 2$ the state transition matrix will be:

$$P_{\{m=2\}} = \begin{array}{c} (\boldsymbol{Z}_n \backslash \boldsymbol{Z}_{n+1}) \\ [0\,0] \\ [0\,1] \\ [1\,0] \\ [1\,1] \end{array} \begin{array}{c} \begin{array}{cccc} [0\,0] & [0\,1] & [1\,0] & [1\,1] \end{array} \\ \begin{pmatrix} 1-p & 0 & p & 0 \\ 1-p & 0 & p & 0 \\ 0 & 1-p & 0 & p \\ 0 & 1-p & 0 & p \end{pmatrix} \end{array}$$

In the above example, E^h and E^l are mapped to 0 and 1 values, respectively. We note that for dated memory, we have $K_n = |\boldsymbol{Z}_n|$, i.e., K_n represents the total number of E^h elements in memory vector $\boldsymbol{Z}_n$.

Results

Distinct timescales of memory-driven phenotypic adaptation to periodic environments affect cellular benefit. We first studied how a cell with either undated or dated memory responds to periodic environmental fluctuations with negligible adaptation cost. In a periodic environment with period T, the cell's estimate of the average environment ($\pi_n \sim \mathbb{P}\left(E_n = E^h\right)$) also varies periodically with the same period as the environment (SI Sec. 4.1.2 and 4.2.2, Figure 2Ai). Clearly, the dynamics of cellular memory (π_n) for dated memory are deterministic since the order of memory loss is completely defined by ordered environmental experiences (gray line in Figure 2Aii). A consequence of deterministic changes in π_n is it can disable cell-state adaptations if the cell memory can not accumulate/dissipate required number of environment exposure in a given period (SI

Sec. 7.2.2). In contrast, randomness in the deletion of previous memories for undated memory limits π_n to exactly follow periodic changes in the environment, thereby leading to the time-varying probability distribution of π_n (Figure 2Aii dashed black line; Figure 2Aiii). Such probabilistic changes in π_n allows for cell-state adaptations even in cases where deterministic changes (from dated memory) disables them, albeit with long waiting times.

Next, we quantified the mean adaptation time to acquiring the preferred phenotype in the current environmental state, and its effect on average cell benefit (SI Sec. 2.3, 7.2.2 and 8). We initially set $p_I = 0.5$, which makes residing in either cell state S^h or S^l equally beneficial on average, given the equal duration of E^h and E^l environments in a period. We found that the dynamics for each memory type depended on the oscillation period (T) and memory capacity (m). For $T \leq m$, memory capacity is large relative to the period of environmental oscillations, enabling cells to accurately measure the entire environmental landscape. Thus, adaptation is disabled/slowed down with extended residence in one of the cell states, allowing the cell to gain optimal benefit from one-half of the period and sub-optimal benefit from the other half (Figure 2B top panel, Figure 2C, Figure S2Aii). On the other hand, having $T >> m$ floods the cell memory with the current environmental state of the period, and therefore, helps in quick cell-state adaptations and enables the cell to gain optimally from both halves of the periods (Figure 2B bottom panel, Figure 2C, Figure S2Aii). Intermediate values of period T with respect to memory capacity m ($T > m$) give mean adaptation times close to one-half of the period. Thus, cell-state adaptations happen when the current environmental state is about to change, causing the cell to be in sub-optimal states for most of the next environmental cycle and consequently, gain suboptimal benefits at all times (Figure 2B middle panel, Figure 2C, Figure S2Aii).

Next, we examined how cellular adaptation changed when we bias a cell state over the other for its average benefit. On making S^h cell state to be more beneficial than S^l on average in the periodic environment, by setting $p_I = 0.3$, we find a large region of memory capacity m and period T that disables/slows down S^h to S^l switch during E^l environmental cycle of the period while enabling/enhancing S^h to S^l switches during E^h environmental cycle of the period (Figure S1). Thus, the cell remains in S^h state and reaps optimal benefit during the E^h environmental cycle and suboptimal benefit during the E^l environmental cycle (Figure S2A). Only when $T >> m$ does adaptation to S^l state fasten up, and the cell benefits optimally from both halves of the environment (Figure S1, Figure S2A). Similar but opposite trends were observed when S^l cell state was more beneficial than S^h on average (by setting $p_I = 0.7$) in the periodic environment (Figure S1, Figure S2A).

Although, the dynamics of both the memory types lead to non-monotonic changes in average benefit with increasing period T for a given memory capacity m, the scale of maximal benefit reduction and its corresponding T value differ between the two memory types (Figure 2C). Such differences lead to regions of T and m values where undated memory is more beneficial than dated memory, and vice versa (Figure 2D, Figure S2B).

Overall, cellular response to an oscillating environment relies on both the memory type and timescales of environmental fluctuations with respect to memory capacity.

Cost of adaptation could prevent maladaptation in periodic environment. Here, we relaxed the cost-free assumption for phenotypic adaptations. We began our analysis with setting $T = 14$ and memory capacity $m = 10$, as the combination enables phenotypic adaptations for both memory types (Figure S1). Perhaps intuitively, increasing adaptation costs restricts adaptation by Eq. (2), which, if such action prevents a switch to the optimal phenotype, must be accompanied by a reduction in the average benefit in a periodic environment (eq. S10). And, in line with the above intuition, we observed decreasing average benefit for increasing adaptation costs in both dated and undated memory types (Figure 2F along the rows, Figure S3). Specifically, with dated memory, we observed that increasing adaptation cost increases maladaptation (environment-phenotype mismatch), thereby reducing the average benefit of the cell (Figure 2E, Figure S3). Maladaptation occurs because, with the adaptation cost, a cell must experience repeated exposure of the current environment before it chooses to adapt compared to no cost adaptation. This requirement effectively delays adaptation and reduces the amount of time the cell phenotype matches the its environment. Similar observations were made with undated memory, where increasing adaptation cost reduced the cell's probability of being in the optimal state for the current environmental state, lowering the cell's average benefit (Figure 2E, Figure S3).

Perhaps surprisingly, large adaptation costs improve a cell's average benefit for both dated and undated memory types (Figure 2F along the rows, Figure S3). Notably, a high cost of adaptation disabled cellular adaptation with dated memory and completely prevented maladaptation to one-half of the environment period, conferring enhanced average benefit as compared to low-to-intermediate cost scenarios (SI Sec. 7.2.2, Figure 2E green solid line, Figure S3). And for undated memory, we found that large adaptation cost increased the chance of environment-phenotype match at the start of the other half of the environmental cycle, thereby balancing the detrimental effect of being in a suboptimal cell state in the current environmental state (Figure 2E, Figure S3).

Following above observation in a specific case, we next proceeded to study how time period T and memory capacity m affect the ability of adaptation costs to influence benefit accrual (Figure 2F and Figure S4). For dated memory, and in regime of short time period ($T \leq m$), cellular adaptation is disabled either at zero or minimal adaptation cost (Figure 2F, grid points with rectangular boxes). In this regime, additional adaptation penalties do not impact the average benefit. In the regime of intermediate periods ($m < T < 2m$), large adaptation cost reduce cellular benefit by delaying adaptation; however, cost beyond a threshold disabled the adaptation with a concomitant rise in average benefit. For environments that

DRAFT

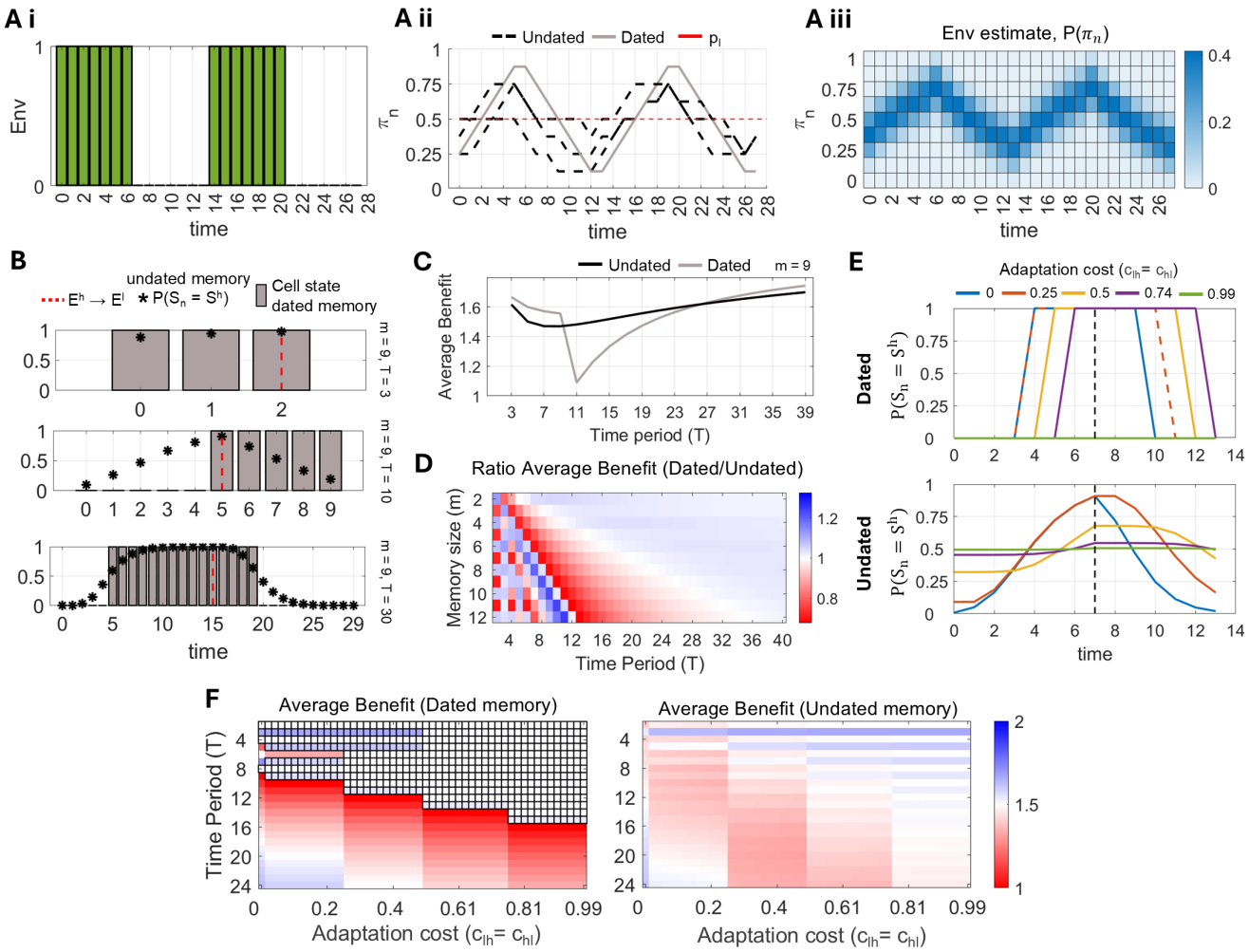

Fig. 2. Cellular response to periodic changes in the environment. **A)** Cell's estimate of the average environment ($\pi_n \sim \mathbb{P}\left(E_n = E^h\right)$) using dated and undated memory. Ai) Example of periodic environment with time period $T = 14$. Aii) Cell's estimate of average environment - deterministic estimate with dated memory and stochastic estimate with undated memory. Aiii) Periodicity in the probability distribution of π_n with undated memory. **B)** Examples of adaptation/maladaptation of cell state from undated and dated memory models for three distinct time periods and fixed memory size. In a time period, the switch in the environment from E^h to E^l is marked by dashed red line.**C)** Variation of average cell benefit with environment period, T for a fixed memory capacity ($m = 9$). **D)** Ratios of average benefit from dated to undated memory for increasing environment period, T, and memory capacity, m, highlight regions where the memory types are optimal. Grid points with black boundaries highlight combinations of T and m where dated memory disables cellular adaptation. **E)** Increasing adaptation cost limits environment-phenotype match. Analysis is done for $m = 10$ and $T = 14$. In the time period, the switch in the environment from E^h to E^l is marked by dashed black line. **F)** Relative value of time period T with respect to cell memory size m ($= 8$) determines the average cell benefit for increasing adaptation cost ($c_{lh} = c_{hl}$). Grid points with black boundaries highlights combinations of period T and adaptation cost ($c_{lh} = c_{hl}$) where dated memory disables cellular adaptation. For all the analyses $p_I = 0.5$ and memory size $m = 10$, unless stated otherwise.

oscillate slowly relative to memory size ($T \geq 2m$), cellular adaptation occurred for all permissible levels of adaptation costs, and therefore, increasing cost always has a detrimental effect on the average benefit. Thus, the range of cost values in which the cost of adaptation was beneficial to the cell shrunk as the memory capacity becomes small relative to the period of the oscillating environment.

Repeating the analysis for the undated memory case demonstrated similar trends in the average benefit. One notable difference was that increasing adaptation cost initially resulted in a decline followed by a ultimate increase in growth benefit for higher costs (Figure 2F, Figure S3, Figure S4). Such non-monotonic nature of the cell's benefit with increasing cost could be explained by the higher probability for the cell to be in the optimal state in the upcoming half of the environmental cycle for very high costs (Figure 2E).

Altogether, the beneficial/detrimental effect of adaptation costs on cellular benefit in an oscillating environment relies on both the memory type and timescales of the environmental fluctuations with respect to memory capacity.

Costly adaptation prevent erroneous state switching in stochastic environment. Having observed that dated and undated memories resulted in distinct cell memory dynamics and growth benefit in a periodic environment, we next explored how dated and undated memories responded to stochastic changes in the environment and their consequences on cellular adaptation.

In the stochastic environment, the probability distribution of cell inference of the environment, π_n, follows a binomial distribution with mean p and variance $\frac{p(1-p)}{m}$ for both the dated and undated memory types (SI Sec. 4.1.1 and 4.2.1, Figure 3A, Figure S6). Thus, with negligible adaptation cost, both

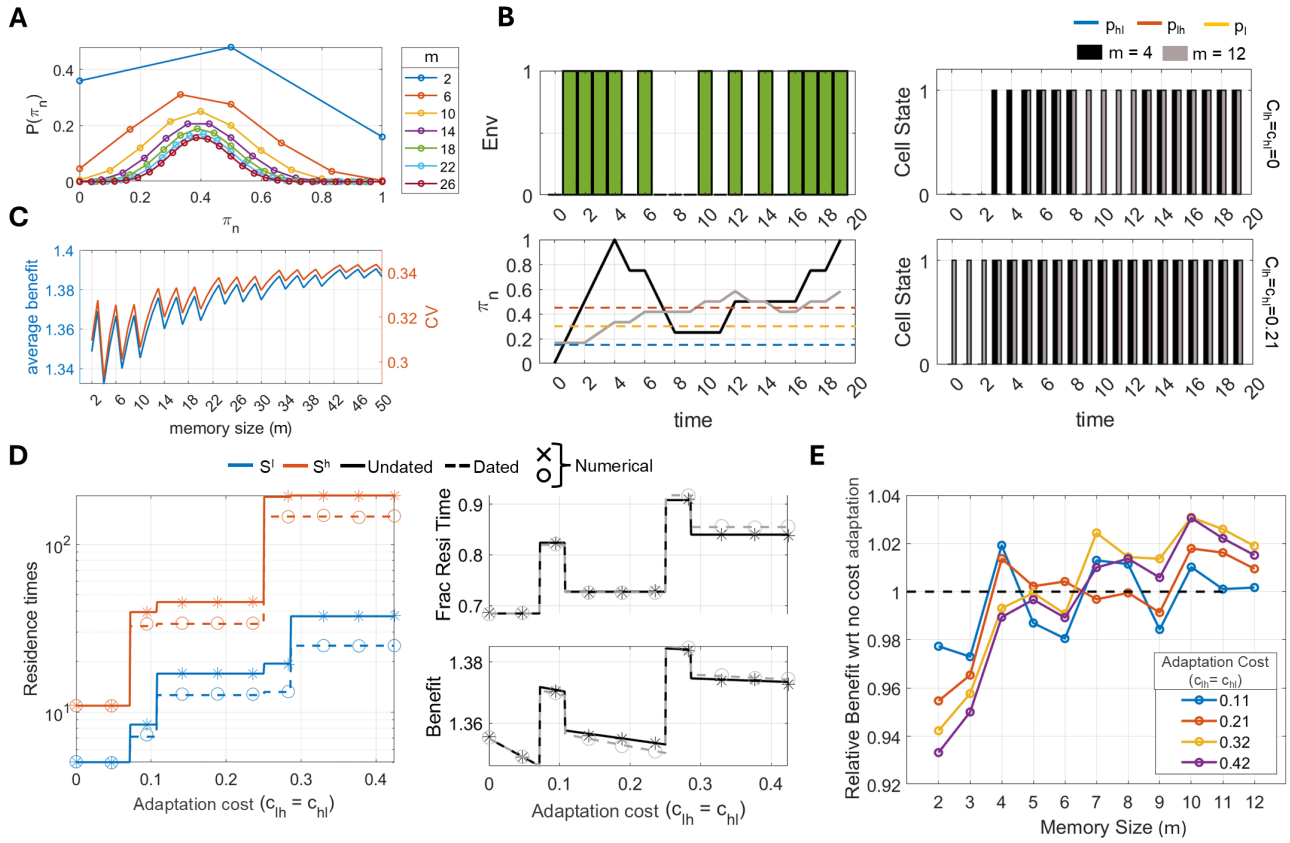

Fig. 3. Cellular response to stochastic changes in the environment. **A)** Larger memory capacity (m) reduce uncertainty in the cell's estimate of the average environment ($\pi_n \sim p = 0.4$). **B)** Presence of adaptation cost reduces fluctuation in the phenotypic states caused due to poor estimate of average environment. Comparison of cell's estimate of average environment (bottom left) and concomitant phenotypic switching with dated memory for small and large memory capacity, with and without adaptation cost (right panels). **C)** Larger memory capacity provides higher average benefit to the cell. Plot also depicts changes in the coefficient of variation (ratio of standard deviation of benefit to its average) with memory size (m). Results obtained with undated memory. **D)** Adaptation cost enhances the residence time in phenotypic states (S^h and S^l) and delays phenotypic switching; increase in fraction of residence time ('Frac Resi time') in optimal phenotypic state (here, S^h), and average cell benefit with adaptation cost. **E)** Identification of lower threshold on memory capacity (m) required for cellular decision making to benefit more from costly adaptation than no cost of adaptation. The observed fluctuations in short intervals of memory capacity in panels C to E are due to the discrete nature of cell memory and points of cellular decision making ($\lfloor p_I m \rfloor$, $\lfloor p_{lh} m \rfloor$, and $\lfloor p_{hl} m \rfloor$). For all the analysis presented above $p = 0.4$, $p_I = 0.3$, $c_{lh} = c_{hl} = 0.21$, and $m = 8$, unless stated otherwise.

memory types lead to equal residence times in cell states S^h and S^l and confer equal average benefits (Figure S10A). Further, since small memory capacity leads to high variance in π_n, we observe erroneous state switching upon cell experiencing a sequence of E^h or E^l by random chance in the recent past (Figure 3B). This erroneous state switching, in turn, reduces the average benefit of the cell, as shown with undated memory (Figure 3C, Figure S6). The above behaviors contrast with periodic environments, where memory types confer distinct average benefits and higher benefits were obtained with smaller memory capacities (Figure 2D and Figure S2A).

In the presence of adaptation costs, increased separation of the decision making point p_{lh} and p_{hl} enhances the mean residence time in both S^h and S^l cell states, thereby reducing cell state transitions (SI Sec. 5, Figure 3B bottom panels and Figure 3D, Figure S7). Specifically, adaptation costs increase the fraction of time spent in the preferred phenotypic state appropriately matched to the environment. This behavior increases average cell benefit (Figure 3D, Figure S7). Thus, in contrast with a periodic environment, we observe an increasing trend in the average benefit with increasing adaptation cost for both the memory types. However, a lower threshold on memory capacity exists, above which costly adaptations are beneficial. Memory capacities below the threshold size result in a great frequency of state switching, which penalizes the cell more than the long-term benefit of adaptation cost (Figure 3E, Figure S8).

Thus, in stochastic environment, both memory types are equally beneficial to the cell, with benefits increasing with adaptation cost.

Dated memory responds faster than undated memory to environmental perturbations. The previous sections detail cellular response in stationary environments, for which T and p are fixed. However, cellular responses to changes in environmental dynamics represent an important scenario that adapting cellular systems must effectively navigate. To study this behavior, we focused on changes in stochastic environments and assumed that the length of time of initial environmental exposure $\mathbb{P}\left(E_n = E^h\right) = p_1$ was large relative to memory capacity. We then assumed that the environment undergoes a sudden transition, governed by $\mathbb{P}\left(E_n = E^h\right) = p_2$. Assuming $p_1 = 0 < p_I = 0.3$, i.e., all en-

vironmental experiences were of E^l making the cell to reside in S^l state, we determine $P(S_n = S^h)$ and adaptation time to S^h state after the environment switch to $p_2 > p_I$ (SI Sec. 7.2.1).

For both dated and undated memory, we observed faster adaptation ($S^l \rightarrow S^h$) whenever the environmental state (p_2) is well-resolved from the indifference environment (that is, $p_2 - p_I$; see Figure 4B, C). This is because in the case of large differences, the average fraction of encountered E^h environmental signals in the memory window (driven by p_2) is much larger than is required (p_I) to undergo a $S^l \rightarrow S^h$ switch, and therefore, this new environment promotes swift adaptation. Similarly, adaptation times are shorter with reduced memory sizes. Furthermore, dated memory has shorter adaptation times than undated memory across memory sizes, and $p_2 - p_I$ values (Figure 4C).

To explain the dependence of adaptation times on memory size, and rapidity of dated memory to environment changes, we quantified how quickly the memory of past environment characteristics (p_1) got replaced with experiences from the current ones (p_2) using the autocorrelation function (SI Sec. 7.1, Figure 4D). We observed larger autocorrelation lengths for increasing memory sizes, thus explaining increase in adaptation time with memory size. Further, dated memory exhibits reduced autocorrelation lengths when compared to undated memory, and therefore, refreshes more rapidly than the latter case, leading to faster adaptation when there is a sudden change in the underlying environment.

Overall, the dated memory provides faster adaptation than undated memory to environmental state changes, with dependence of mean adaptation times on the memory capacity and resolution of current environmental state (p_2) with indifference environment (p_I).

Costly transition delays adaptation on abrupt environment switches. So far, we have observed beneficial and detrimental effects arising from costly phenotypic adaptation in stationary environments. However, the previous observations did not capture the effects of costly adaptation on transient cellular responses. Since costly adaptation shifts the indifference environment values and restricts cellular adaptation Eq. (2), we expected that costly adaptations would increase the time to adapt to the environment. To evaluate this, we again considered perturbations in environmental state from p_1 to p_2, following $p_1 < p_I < p_2$, and determined the mean time to attain S^h cell state with increasing adaptation costs. We found that increasing adaptation costs further delayed cellular adaptation to the new environment, transiently reducing the average benefit to the cell just after the environmental shift (Figure 4E, F). Our findings suggest that, even though adaptation costs can benefit the cells in stationary environments, they are always detrimental in the short run whenever there is a systematic shift in the underlying state of environmental fluctuations.

Discussion

Cells must continually adapt to fluctuations in their environments by making phenotypic choices that enhance their growth or survival, or result in desirable actions (migration toward a nutrient source). Previous studies had contributed fundamental insights on - 1) when active sensing and related adaptation would be more beneficial than bet-hedging (13), 2) the optimal rates of spontaneous cell state switching as a function of environmental fluctuations (12), and 3) the tradeoff between survivability in adverse environments and growth recovery rate in favorable ones (11). Studies on cellular adaptation at the individual cell level has identified negative feedback loops as a conserved feature leading to active turnover of biomolecules and a homeostatic need for energy influx (31, 32). However, complexity of these biochemical networks limits their detailed analysis in fluctuating environments, and therefore, require phenomenological approaches for their characterization (10, 16, 17). In this study, by developing a foundational models of cellular memory, we have elucidated how single-step (undated) vs multi-step (dated) decay of past experiences and adaptation cost together influence cell state switching and growth in fluctuating environments (Figure 1).

In the dated memory, each experience gets erased from memory after m definite time steps. This memory structure imposes a strong constraint and may deviate from a realistic scenario where the timings of biomolecule degradation, after multi-step processing, can be stochastic. Nonetheless, our dated memory model accurately captures the time dynamics of an explicit multi-step (non-exponential) decay model of bio-molecules as both of them resulted in linearly decreasing autocorrelation function with increase in time lags (38) (Figure 4D).

Our above framework assumes finite memory capacity ($m < \infty$) and thus makes imperfect inference of any given environment, since perfect inference in our model would require infinite time and unbounded capacity. One can also estimate the memory capacity of a biochemical reaction network through protein abundances, either by direct measurements or using proxies, such as the codon adaptation index (39, 40). However, in all our analyses, we have set memory capacities to arbitrary small values $m(\leq 12)$ because of cell memory dynamics giving very long residence times in cell states either for larger memory capacities or for high adaptation costs (Figure 3D and Figure S9). Nonetheless, our range of memory capacity captured its non-intuitive roles in driving cellular adaptations in fluctuating environments (Figure 2B, D; Figure 3C, E).

We observed that sequential decay of past environmental experience with dated memory resulted in fast turnover of the cell memory (Figure 4D), and therefore caused the cell to - 1) adapt quickly to single-transitions in the environment (Figure 4B), and 2) cycle fast between cell states under costly adaptation in stochastic environments as compared to undated memory (Figure S10). Although rapid turnover and cell state cycling from dated memory were more beneficial to cells undergoing single-environment transitions over adaptation with

DRAFT

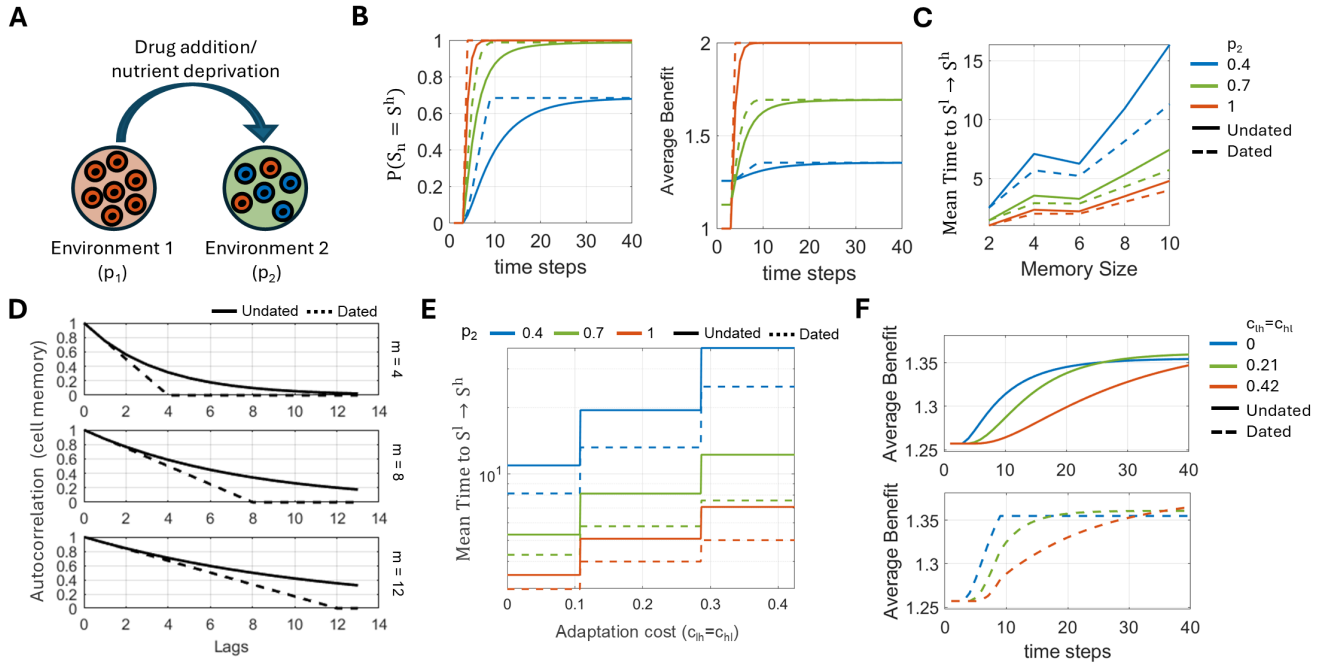

Fig. 4. Cellular response to abrupt change in the environmental state. **A)** Schematic representation of change in stochastic environmental state from p_1 to p_2 and the resulting phenotypic adaptation. **B)** Rate of phenotypic adaptation scales with increasing resolution between indifference environment and new environmental state ($|p_2 - p_I|$). Changes in the probability of cell being in optimal state, and concomitant increase in average benefit over time when environmental state switches from $p_1 = 0$ to $p_2 = \{0.4, 0.7, 1\}$ for $p_I = 0.3$. **C** Delayed cellular adaptation with larger cell memory capacity (m). Quantification of mean time to attain S^h on environmental switch for increasing memory capacity and increasing p_2 values. **D)** Autocorrelation of cell's estimate of environment, π_n, shows that the remembrance of past environmental experiences increase with memory size and is short-lived for dated memory than undated memory; and **E)** Adaptation cost delays adaptation to the preferred state S^h on environmental switch, and the delays scales up with smaller magnitude of $(p_2 - p_I)$ **F)** Increasing adaptation cost reduces the short-term cumulative average benefit on environmental switch. For all the analysis presented above $p_1 = 0$, $p_2 = 0.4$, $p_I = 0.3$, and $m = 8$, unless stated otherwise.

undated memory (Figure 4B), their utility to cellular benefit in stochastic environments was not evident (Figure 3D). Intriguingly, in the periodic environment, rapid turnover (sequential decay) of dated memory results in significant delays in cellular adaptation. Dated memory is therefore suboptimal for the cell when the period of the environment was just greater than memory size (Figure 2D). Thus, our analysis predicts that the optimal memory type (with one-step vs multi-step decay) depends on the characteristic fluctuation of the environment, and whether or not they are deterministic or stochastic. This suggests individual stress response pathways might have evolved to either have one-step or multi-step decay/relaxation time of their component bio-molecules, depending on the fluctuation characteristics of the corresponding stressor.

A few recent experimental studies observed the existence of cellular memory in periodically fluctuating environments and measured the effect of cellular memory on the growth of the population (4, 5, 19). Nguyen et al. observed distinct cellular state in a fluctuating environment whose growth rate was smaller than the average of cellular growth in two static environments (4). Further, the authors also observed non-monotonic changes in growth rates with increasing periods of environmental fluctuations. The model developed here successfully recapitulated the above empirical observations (Figure S5A). Another observation made with periodic environmental fluctuations is of growth reversal, whereby environment fluctuations reduce (resp. enhance) growth in environments with higher (resp. lower) static benefit (5). We set up an equivalent scenario of two environments with unequal static benefits (by offsetting p_I from 0.5), and compared cellular adaptation and benefit in static vs oscillating environments. While fluctuating environments reduced benefit in the environment with higher static benefit, which aligns with the experimental observation, we did not observe fluctuating environments enhancing growth benefits in the environment with lower static benefit (Figure S5B). Since the growth reversal was observed with evolved bacterial cells in either static or fluctuating environments over multiple generations, we must account for the possibility of differential mutations and their effects on cellular adaptation in order to explain long-term evolutionary experiments in static vs fluctuating environments (5).

Our analysis with cost of adaptation in fluctuating environment showed that, counterintuitively, the addition of adaptation costs could improve cellular decision making in stochastic and periodic environments and also enhance long-term growth benefit (Figure 2F and Figure 3D). Particularly, in stochastic environments, costly adaptations achieved higher growth benefit due to a larger fraction of time spent in cell state optimally matched to the environment (Figure 3D). In periodic environments, high adaptation costs achieved higher growth benefits by reducing cell-state switching and by balancing (dis-)advantages of environment-phenotype (mis-)match on every environment cycle (Figure 2E and Figure S3). However, in single-step environmental transitions, adaptation cost reduced adaptation speed and also short-term cumulative growth benefit (Figure 4E,F). Since adaptation costs

DRAFT

relate to energetic costs for *de-novo* synthesis of essential bio-molecules, our observations above suggests the intriguing possibility of evolutionary strategies that impose an adaptation cost in order to enhance the benefit of a fluctuating environment. We remark that a heterogeneous population of cells having a distribution of memory-specific biomolecule levels would contribute further cell-cell variability in the cost of adaptation. Therefore, in a population of cells with distributed adaptation costs, we would observe a distribution of adaptation times for cells navigating single-step and periodic environmental transitions with some cell adapting faster than the others (Figure 4E,F). Such a scenario is directly relevant to a number of biological contexts. For example, drug persister cells have reduced adaptation costs relative to other cells in the ecology, which helps them to quickly adapt and survive in the sudden drug presentation (single-step transition) (41–43). Further, our analysis with periodic environments predicts that reduced adaptation costs of persister cells can lower their long-term growth benefit if the environmental period is of the order of memory capacity ($T \leq 2m$). This result is consistent with greater efficacy obtained in adaptive dosing strategies (44) and offers a quantitative means by which optimal treatment cycles can be identified based on experimental tests to probe the memory capacity underlying adaptation in a given cancer context.

Our model helps us realize key similarities and differences between spontaneous state switching and cellular memory-driven cellular adaptations. In an oscillating environment, both spontaneous switching and memory-driven adaptations rely on optimal state switching to maximize cellular benefit. However, while spontaneous switching-based population adaptation may optimize switching rates entirely based on environmental fluctuation characteristics, memory-driven adaptation relies on adaptation cost and memory capacity in addition to environmental characteristics to optimize switching rates (12) (Figure 2). Moreover, memory-driven adaptations in stochastic environments confer maximal benefit by minimizing cell-state switching irrespective of environment uncertainty, which is opposed to spontaneous switching-based population adaptation in stochastic environments (13) (Figure 3). The above similarities and differences lead to several open questions – 1) Under what conditions growth from memory-driven adaptation will exceed growth from spontaneous switching-based adaptation?, 2) How could one account for the cost of adaptation/state switching under spontaneous state transitions and whether adaptation/switching cost affect spontaneous switching rates?, and 3) Whether or not cellular changes under spontaneous switching a subset of extensive changes that occur on memory-driven adaptation? (9). An iterative and integrated experimental and modeling effort may help us to answer the above questions.

There are a few key limitations of this work - First of all, the discrete time nature of the cell memory model limits their quantitative match with experimental timescales (4, 5, 45). Model extension to continuous time will help to address these challenges. In the developed cell memory models, we assumed that each environmental encounter is recorded as such in the cell memory. Signaling pathways that exhibit a step-like response to external ligand concentration below and above the threshold represent appropriate biological contexts for this assumption (23, 46). However, signaling responses are often graded instead of step-wise, and they may variably respond to either instantaneous concentration, fold change in concentration, or a temporal gradient of their associated ligands (46–48). Although we limited our scope to study the effects of how past cellular experience decay, subsequent studies that consider the precise encoding of cellular memory and how those choices impact cellular adaptation through memory decay will be an important follow-up task (45). Lastly, we assumed discrete cell states with transitions between them being purely governed by past environmental experiences. However, cell states are far from being discrete because of stochasticity in intracellular biochemical reactions (49, 50). Such subtle difference in cell states may contribute to survival of a fraction of cells in the event of environment change (41, 51, 52). Although, population-level variability in adaptation costs as discussed above can capture this cell-cell variability, an explicit account of stochastic state switching along with active sensing in a single model could be more informative for their combined effects on cellular adaptation and long-term growth benefits in fluctuating environments (53). Nonetheless, our phenomenological framework offers key insights on the the effects of cell memory and adaptation costs on cellular adaptations in fluctuating environments. These results contribute to our understanding of how complexity in intracellular processes shape cellular responses to changing environments.

DRAFT

AUTHOR CONTRIBUTIONS

P.J., M.K.J, and J.T.G. conceived of and designed the research. P.J. performed the research. P.J., M.K.J., and J.T.G contributed new analytic equations, analyzed the results, and wrote the paper. J.T.G. and M.K.J. supervised the research.

COMPETING FINANCIAL INTERESTS

The authors declare no competing interests.

ACKNOWLEDGEMENTS

M.K.J. and P.J. were supported by Param Hansa Philanthropies. J.T.G. was supported by the Cancer Prevention Research Institute of Texas (RR210080) and the National Institute of General Medical Sciences of the NIH (R35GM155458). J.T.G. is a CPRIT Scholar in Cancer Research.

Data and Code Availability

The code files for numerical evaluations of the formulations developed in this study can be found at:

https://github.com/Paras-Jain20/Memory-and-cost-in-cellular-adaptation

Bibliography

1. Jacques Monod. The growth of bacterial cultures. *Selected Papers in Molecular Biology by Jacques Monod*, 139:606, 2012.
2. David W Erickson, Severin J Schink, Vadim Patsalo, James R Williamson, Ulrich Gerland, and Terence Hwa. A global resource allocation strategy governs growth transition kinetics of escherichia coli. *Nature*, 551(7678):119–123, 2017.
3. Sreenath V Sharma, Diana Y Lee, Bihua Li, Margaret P Quinlan, Fumiyuki Takahashi, Shyamala Maheswaran, Ultan McDermott, Nancy Azizian, Lee Zou, Michael A Fischbach, et al. A chromatin-mediated reversible drug-tolerant state in cancer cell subpopulations. *Cell*, 141 (1):69–80, 2010.
4. Jen Nguyen, Vicente Fernandez, Sammy Pontrelli, Uwe Sauer, Martin Ackermann, and Roman Stocker. A distinct growth physiology enhances bacterial growth under rapid nutrient fluctuations. *Nature Communications*, 12(1):3662, 2021.
5. Clare I Abreu, Shaili Mathur, and Dmitri A Petrov. Environmental memory alters the fitness effects of adaptive mutations in fluctuating environments. *Nature Ecology & Evolution*, 8(9): 1760–1775, 2024.
6. Roman Stocker. Marine microbes see a sea of gradients. *science*, 338(6107):628–633, 2012.
7. Tom Fenchel. Microbial behavior in a heterogeneous world. *Science*, 296(5570):1068–1071, 2002.

8. Katherine L Eales, Kate ER Hollinshead, and Daniel A Tennant. Hypoxia and metabolic adaptation of cancer cells. *Oncogenesis*, 5(1):e190–e190, 2016.
9. Jingxin Li, Pavithran T Ravindran, Aoife O'Farrell, Gianna T Busch, Ryan H Boe, Zijian Niu, Sean Woo, Margaret C Dunagin, Naveen Jain, Yogesh Goyal, et al. Ap-1 mediates cellular adaptation and memory formation during therapy resistance. *bioRxiv*, 2024.
10. Jason T George. Optimal phenotypic adaptation in fluctuating environments. *Biophysical Journal*, 122(22):4414–4424, 2023.
11. Nico Geisel, Jose MG Vilar, and J Miguel Rubi. Optimal resting-growth strategies of microbial populations in fluctuating environments. *PLoS One*, 6(4):e18622, 2011.
12. Edo Kussell, Roy Kishony, Nathalie Q Balaban, and Stanislas Leibler. Bacterial persistence: a model of survival in changing environments. *Genetics*, 169(4):1807–1814, 2005.
13. Edo Kussell and Stanislas Leibler. Phenotypic diversity, population growth, and information in fluctuating environments. *Science*, 309(5743):2075–2078, 2005.
14. Gerardo Aquino, Luke Tweedy, Doris Heinrich, and Robert G Endres. Memory improves precision of cell sensing in fluctuating environments. *Scientific reports*, 4(1):5688, 2014.
15. Gary Friedman, Stephen McCarthy, and Dmitrii Rachinskii. Hysteresis can grant fitness in stochastically varying environment. *PLoS One*, 9(7):e103241, 2014.
16. Stefan Legewie, Dennis Dienst, Annegret Wilde, Hanspeter Herzel, and Ilka M Axmann. Small rnas establish delays and temporal thresholds in gene expression. *Biophysical journal*, 95(7):3232–3238, 2008.
17. Elizabeth R Westbrook, Hugh Z Ford, Vlatka Antolović, and Jonathan R Chubb. Clearing the slate: Rna turnover to enable cell-state switching? *Development*, 150(19), 2023.
18. Eitan Rotem, Adiel Loinger, Irine Ronin, Irit Levin-Reisman, Chana Gabay, Noam Shoresh, Ofer Biham, and Nathalie Q Balaban. Regulation of phenotypic variability by a threshold-based mechanism underlies bacterial persistence. *Proceedings of the National Academy of Sciences*, 107(28):12541–12546, 2010.
19. Guillaume Lambert and Edo Kussell. Memory and fitness optimization of bacteria under fluctuating environments. *PLoS genetics*, 10(9):e1004556, 2014.
20. Angela Oliveira Pisco, Amy Brock, Joseph Zhou, Andreas Moor, Mitra Mojtahedi, Dean Jackson, and Sui Huang. Non-darwinian dynamics in therapy-induced cancer drug resistance. *Nature communications*, 4(1):2467, 2013.
21. Stefan Hohmann. Osmotic stress signaling and osmoadaptation in yeasts. *Microbiology and molecular biology reviews*, 66(2):300–372, 2002.
22. Maor Knafo, Shahar Rezenman, Reinat Nevo, Ivgeni Tsigalnitski, Ziv Reich, and Ruti Kapon. Variability in protein expression and fitness under stress: Distinct modes of early adaptation of populations. *PRX Life*, 3(1):013006, 2025.
23. Tanmay Mitra, Shakti N Menon, and Sitabhra Sinha. Emergent memory in cell signaling: Persistent adaptive dynamics in cascades can arise from the diversity of relaxation timescales. *Scientific Reports*, 8(1):13230, 2018.
24. Jette Strasen, Uddipan Sarma, Marcel Jentsch, Stefan Bohn, Caibin Sheng, Daniel Horbelt, Petra Knaus, Stefan Legewie, and Alexander Loewer. Cell-specific responses to the cytokine tgf β are determined by variability in protein levels. *Molecular systems biology*, 14 (1):e7733, 2018.
25. M Violet Lee, Scott E Topper, Shane L Hubler, James Hose, Craig D Wenger, Joshua J Coon, and Audrey P Gasch. A dynamic model of proteome changes reveals new roles for transcript alteration in yeast. *Molecular systems biology*, 7(1):514, 2011.
26. Daniel H Lackner, Michael W Schmidt, Shuangding Wu, Dieter A Wolf, and Jürg Bähler. Regulation of transcriptome, translation, and proteome in response to environmental stress in fission yeast. *Genome biology*, 13:1–14, 2012.
27. Carlus Deneke, Reinhard Lipowsky, and Angelo Valleriani. Complex degradation processes lead to non-exponential decay patterns and age-dependent decay rates of messenger rna. *PloS one*, 8(2):e55442, 2013.
28. Don Benjamin, Marco Colombi, Georg Stoecklin, and Christoph Moroni. A gfp-based assay for monitoring post-transcriptional regulation of are-mrna turnover. *Molecular Biosystems*, 2(11):561–567, 2006.
29. Erik McShane, Celine Sin, Henrik Zauber, Jonathan N Wells, Neysan Donnelly, Xi Wang, Jingyi Hou, Wei Chen, Zuzana Storchova, Joseph A Marsh, et al. Kinetic analysis of protein stability reveals age-dependent degradation. *Cell*, 167(3):803–815, 2016.
30. Alison Barbara Ross, Julian David Langer, and Marko Jovanovic. Proteome turnover in the spotlight: approaches, applications, and perspectives. *Molecular & Cellular Proteomics*, 20: 100016, 2021.
31. Ganhui Lan, Pablo Sartori, Silke Neumann, Victor Sourjik, and Yuhai Tu. The energy–speed–accuracy trade-off in sensory adaptation. *Nature physics*, 8(5):422–428, 2012.
32. Wenzhe Ma, Ala Trusina, Hana El-Samad, Wendell A Lim, and Chao Tang. Defining network topologies that can achieve biochemical adaptation. *Cell*, 138(4):760–773, 2009.
33. Pankaj Mehta and David J Schwab. Energetic costs of cellular computation. *Proceedings of the National Academy of Sciences*, 109(44):17978–17982, 2012.
34. Santiago Sandoval Motta, Philippe Cluzel, and Maximino Aldana. Adaptive resistance in bacteria requires epigenetic inheritance, genetic noise, and cost of efflux pumps. *PloS one*, 10(3):e0118464, 2015.
35. Daniel M Stoebel, Antony M Dean, and Daniel E Dykhuizen. The cost of expression of escherichia coli lac operon proteins is in the process, not in the products. *Genetics*, 178(3): 1653–1660, 2008.
36. Joel G Belasco. All things must pass: contrasts and commonalities in eukaryotic and bacterial mrna decay. *Nature reviews Molecular cell biology*, 11(7):467–478, 2010.
37. Hayun Lee and Dipali G Sashital. Creating memories: molecular mechanisms of crispr adaptation. *Trends in biochemical sciences*, 47(6):464–476, 2022.
38. Juan M Pedraza and Johan Paulsson. Effects of molecular memory and bursting on fluctuations in gene expression. *Science*, 319(5861):339–343, 2008.
39. Peng Lu, Christine Vogel, Rong Wang, Xin Yao, and Edward M Marcotte. Absolute protein expression profiling estimates the relative contributions of transcriptional and translational regulation. *Nature biotechnology*, 25(1):117–124, 2007.
40. Paul M Sharp and Wen-Hsiung Li. The codon adaptation index-a measure of directional synonymous codon usage bias, and its potential applications. *Nucleic acids research*, 15 (3):1281–1295, 1987.
41. Sydney M Shaffer, Margaret C Dunagin, Stefan R Torborg, Eduardo A Torre, Benjamin Emert, Clemens Krepler, Marilda Beqiri, Katrin Sproesser, Patricia A Brafford, Min Xiao, et al. Rare cell variability and drug-induced reprogramming as a mode of cancer drug resistance. *Nature*, 546(7658):431–435, 2017.
42. Benjamin L Emert, Christopher J Cote, Eduardo A Torre, Ian P Dardani, Connie L Jiang, Naveen Jain, Sydney M Shaffer, and Arjun Raj. Variability within rare cell states enables multiple paths toward drug resistance. *Nature biotechnology*, 39(7):865–876, 2021.
43. Tyler Risom, Ellen M Langer, Margaret P Chapman, Juha Rantala, Andrew J Fields, Christopher Boniface, Mariano J Alvarez, Nicholas D Kendsersky, Carl R Pelz, Katherine Johnson-Camacho, et al. Differentiation-state plasticity is a targetable resistance mechanism in basal-like breast cancer. *Nature communications*, 9(1):1–17, 2018.
44. Jingsong Zhang, Jessica J Cunningham, Joel S Brown, and Robert A Gatenby. Integrating evolutionary dynamics into treatment of metastatic castrate-resistant prostate cancer. *Nature communications*, 8(1):1816, 2017.
45. Josiah Kratz, Huijing Wang, Fangwei Si, and Shiladitya Banerjee. Power-law memory governs bacterial adaptation and learning in fluctuating environments. *bioRxiv*, pages 2025–04, 2025.
46. Yaron E Antebi, Nagarajan Nandagopal, and Michael B Elowitz. An operational view of intercellular signaling pathways. *Current opinion in systems biology*, 1:16–24, 2017.
47. Pulin Li, Joseph S Markson, Sheng Wang, Siheng Chen, Vipul Vachharajani, and Michael B Elowitz. Morphogen gradient reconstitution reveals hedgehog pathway design principles. *Science*, 360(6388):543–548, 2018.
48. Benoit Sorre, Aryeh Warmflash, Ali H Brivanlou, and Eric D Siggia. Encoding of temporal signals by the tgf-β pathway and implications for embryonic patterning. *Developmental cell*, 30(3):334–342, 2014.
49. Arjun Raj, Charles S Peskin, Daniel Tranchina, Diana Y Vargas, and Sanjay Tyagi. Stochastic mrna synthesis in mammalian cells. *PLoS biology*, 4(10):e309, 2006.
50. Arjun Raj and Alexander Van Oudenaarden. Nature, nurture, or chance: stochastic gene expression and its consequences. *Cell*, 135(2):216–226, 2008.
51. Sabrina L Spencer, Suzanne Gaudet, John G Albeck, John M Burke, and Peter K Sorger. Non-genetic origins of cell-to-cell variability in trail-induced apoptosis. *Nature*, 459(7245): 428–432, 2009.
52. Yogesh Goyal, Gianna T Busch, Maalavika Pillai, Jingxin Li, Ryan H Boe, Emanuelle I Grody, Manoj Chelvanambi, Ian P Dardani, Benjamin Emert, Nicholas Bodkin, et al. Diverse clonal fates emerge upon drug treatment of homogeneous cancer cells. *Nature*, 620(7974):651–659, 2023.
53. Dino Osmanović, Yitzhak Rabin, and Yoav Soen. A model of epigenetic inheritance accounts for unexpected adaptation to unforeseen challenges. *Advanced Science*, page 2414297, 2025.

DRAFT